

# Broadband Coupling into a Single-Mode, Electroactive Integrated Optical Waveguide for Spectroelectrochemical Analysis of Surface-Confined Redox Couples

John Thomas Bradshaw,<sup>†</sup> Sergio B. Mendes,<sup>‡</sup> Neal R. Armstrong,<sup>†,‡</sup> and S. Scott Saavedra<sup>\*,†</sup>

Department of Chemistry and Optical Sciences Center, University of Arizona, Tucson, Arizona 85721

**A single-mode, electroactive waveguiding platform capable of measuring spectroelectrochemical responses of surface-adsorbed redox-active molecules over a broad spectral bandwidth has been created. This new planar waveguide spectrometer is a combination of the previously developed electroactive integrated optical waveguide (EA-IOW; Dunphy, D. R.; Mendes, S. B.; Saavedra, S. S.; Armstrong, N. R. *Anal. Chem.* 1997, 69, 3086–3094) with a recently reported simplified approach to broadband coupling (Bradshaw, J. T.; Mendes, S. B.; Saavedra, S. S. *Anal. Chem.* 2002, 74, 1751–1759). With the use of a commercially available prism as an incoupling element, the EA-IOW can now guide visible light from at least 500 to 700 nm, improving upon its previously demonstrated monochromatic nature. Coupling profiles of various laser lines along with transmission spectra of narrow band-pass filters at various potentials are used to demonstrate the optical characteristics of this broadband EA-IOW and to compare its response to that of a conventional transmission instrument. Assessment of spectral resolution, performed by measuring the fwhm of various laser lines, ranges from 0.6 to 0.8. To demonstrate the capabilities of this technology, we show the acquisition of absorbance spectra of two different adsorbates, cytochrome *c* and ferrocenedicarboxylic acid, as a function of applied potential. Subtleties in the redox chemistries of adsorbed molecules, which were difficult to monitor with a monochromatic waveguide, are readily apparent when using the broadband coupling scheme.**

Pushing the sensitivity of spectroelectrochemical techniques to routinely monitor changes in spectral properties of thin molecular films (i.e., monolayer or submonolayer) adsorbed on an electrode surface has been a goal of many investigators since the earliest developments in this field.<sup>1</sup> It was initially recognized that exploiting the evanescent field generated by total internal

reflection at the interface of an optically transparent electrode (such as a thin film of tin oxide or indium tin oxide (ITO) on glass or quartz) has the inherent advantage of selectively probing only the near-surface region, as opposed to bulk sampling with transmission based techniques. Furthermore, by utilizing the multiple reflections in an attenuated total reflectance (ATR) geometry, an enhancement in sensitivity can be realized, and as the thickness of the ATR element is decreased, the number of reflections increases, yielding a substantial sensitivity enhancement.<sup>2–6</sup> Itoh and Fujishima were the first to show the advantages of reducing the thickness of an ATR element overcoated with a transparent conductive oxide to the integrated optical waveguide (IOW) regime. Using a four-mode, gradient index waveguide coated with a transparent, conductive tin oxide layer, they demonstrated large sensitivity enhancements, relative to a single pass transmission experiment, for spectroelectrochemical measurements of methylene blue.<sup>7,8</sup> Other research groups subsequently described similar gradient index, multilayer, electroactive waveguide structures, but they did not make use of the technology to explore the spectroelectrochemistry of (sub)monolayer coverage films.<sup>9–13</sup>

We recently described a single-mode, electroactive planar IOW (the EA-IOW) having a step refractive index profile. It was fabricated by sputtering a Corning 7059 glass layer (400 nm) over soda lime glass or quartz, followed by a 200-nm layer of SiO<sub>2</sub>,

- (2) Hansen, W. N.; Osteryoung, R. A.; Kuwana, T. *J. Am. Chem. Soc.* **1966**, *88*, 1062–1063.
- (3) Hansen, W. N.; Kuwana, T.; Osteryoung, R. A. *Anal. Chem.* **1966**, *38*, 1810–1821.
- (4) Winograd, N.; Kuwana, T. *J. Electroanal. Chem.* **1969**, *23*, 333–342.
- (5) Winograd, N.; Kuwana, T. *J. Am. Chem. Soc.* **1971**, *93*, 4343–4350.
- (6) Winograd, N.; Kuwana, T. *Anal. Chem.* **1971**, *43*, 252–259.
- (7) Itoh, K.; Fujishima, A. *J. Phys. Chem.* **1988**, *92*, 7043–7045.
- (8) Itoh, K.; Fujishima, A. In *Electrochemistry in Transition*; Murphy, O. J., Srinivasan, S., Conway, B. E., Eds.; Plenum Press: New York, 1992; pp 219–225.
- (9) Piraud, C.; Mwarania, E.; Wylangowski, G.; Wilkinson, J.; O'Dwyer, K.; Schiffrin, D. J. *Anal. Chem.* **1992**, *64*, 651–655.
- (10) Kremeskoetter, J.; Wilson, R.; Schiffrin, D. J.; Luff, B. J.; Wilkinson, J. S. *Meas. Sci. Technol.* **1995**, *6*, 1325–1328.
- (11) Matsuda, N.; Takatsu, A.; Kato, K.; Shigesato, Y. *Chem. Lett.* **1998**, 125–126.
- (12) Miller, L. W.; Tejedor, I.; Nelson, B. P.; Anderson, M. A. *J. Phys. Chem. B* **1999**, *103*, 8490–8492.
- (13) Ross, S. E.; Seliskar, C. J.; Heineman, W. R. *Anal. Chem.* **2000**, *72*, 5549–5555.

\* To whom correspondence should be addressed. Phone: (520) 621-9761. Fax: (520) 621-8407. E-mail: saavedra@email.arizona.edu.

<sup>†</sup> Department of Chemistry.

<sup>‡</sup> Optical Sciences Center.

(1) Kuwana, T. *Ber. Bunsen-Ges. Phys. Chem.* **1973**, *77*, 858–871.

followed by a 25–50-nm layer of ITO.<sup>14,15</sup> Characterization of this device demonstrated a  $10^3$ – $10^4$ -fold sensitivity enhancement in spectroscopic measurements of adsorbed redox couples versus a conventional single-pass transmission measurement. This high degree of sensitivity, which results from the step index nature of the multilayer EA-IOW design, was subsequently shown to be useful for exploring the redox chemistries of submonolayer molecular films, including films of horse heart cytochrome *c* (cyt *c*), methylene blue, and rodlike molecular assemblies based on axially polymerized or aggregated phthalocyanines.<sup>14,15</sup>

The original EA-IOW was implemented as a monochromatic device, which is an inherent limitation of single-mode, step index, planar waveguides. This limitation arises from the dependence of the effective index of a bound mode on the wavelength of propagating light, as described in detail elsewhere.<sup>16,17</sup> Thus, different wavelengths of light propagate at different internal reflection angles to produce a guided mode for each wavelength. The practical consequence is that, for a given experimental configuration (i.e., optical alignment), an IOW-ATR measurement can be performed at only a single wavelength or at best over a very narrow spectral window, which limits the information content of the experiment.

Attempts to overcome the narrow spectral bandwidth of planar IOWs have been described.<sup>18–24</sup> The first truly successful solutions to broadband coupling were reported by Mendes et al.<sup>25–27</sup> In each case, an incoupling element(s) was used to disperse a broad spectral band of light, incident at a single incoupling angle, into bound waveguide modes<sup>25–27</sup> (vide infra). Within the spectral bandwidth (up to 110 nm), every wavelength was achromatically coupled into its respective waveguide mode with high efficiency. However, these incoupling elements had to be custom fabricated to match a specified planar IOW structure, and in the case of the multicomponent incoupler,<sup>25,26</sup> highly precise alignment was required for the device to operate properly.

More recently, we reported a much simpler broadband coupling approach based on a commercially available, high refractive index prism coupled to a sol–gel glass, single-mode planar IOW.<sup>28</sup> Using this approach, nearly the entire visible

spectrum ( $\sim 250$  nm) could be incoupled and guided at one incident angle. An integral diffraction grating was used to outcouple the guided light and disperse it onto a CCD camera. Although not as efficient as the coupling approaches developed by Mendes et al.,<sup>25–27</sup> the simplified approach allowed multichannel ATR spectra of IOW-supported, submonolayer molecular films to be measured with high sensitivity.

In this paper, we report on the application of the simplified broadband coupling approach to the EA-IOW, which allows a 210-nm band of visible light to be incoupled and guided at one incident angle. Potential-dependent characteristics of broadband coupling into an EA-IOW are described, and the optical performance of an EA-IOW-ATR spectrometer is characterized and compared to that of a commercially available, transmission-based spectrometer. Finally, the utility of this apparatus for measuring potential-dependent ATR spectra of molecular films is demonstrated using adsorbed films of horse heart cytochrome *c* and ferrocenedicarboxylic acid.

## EXPERIMENTAL SECTION

**Waveguide Fabrication.** Design and construction of the EA-IOW has been previously described in detail.<sup>14,15</sup> It is a multi-layered structure consisting of the following: (1) a soda lime glass substrate containing an integral diffraction grating for outcoupling the “waveguided” light, (2) a 400-nm layer of Corning 7059 glass, (3) a 200-nm layer of silicon dioxide, and (4) a 25-nm ITO electrode layer. The diffraction grating was fabricated in the substrate prior to waveguide deposition via a holographic process as described previously.<sup>28–30</sup> The substrate was then coated with the Corning 7059 layer, followed by deposition of the SiO<sub>2</sub> and finally the ITO, using a Perkin-Elmer 2400 rf diode sputtering system. EA-IOW structures were experimentally determined to support both TE<sub>0</sub> and TM<sub>0</sub> modes by assessing guiding characteristics using various laser lines (ranging from 514.5 to 632.8 nm). The estimated propagation loss was 5 dB/cm at 633 nm.<sup>14</sup> Grating period was determined to be  $\sim 400$  nm by measuring the diffraction angle in the Littrow configuration and confirmed by atomic force microscopy (AFM).

**Optical Layout/Electrochemical Cell.** Broadband coupling into the EA-IOW was achieved in the same fashion as the design recently reported from our laboratory for sol–gel glass planar waveguides.<sup>28</sup> The incoupling element used for all experiments was a truncated, right-angle (45–45–90), Schott glass prism (SF6, Karl Lambrecht). Black silicon adhesive was used to mount the incoupling prism into a custom spectroelectrochemical flow cell made from black plexiglass (Figure 1). The EA-IOW was mounted into the flow cell, electrolyte solution was then injected in order to fill the gap between the prism base and the waveguide surface, and pressure was applied to the top of the prism via a mounting clamp to achieve coupling.<sup>28</sup> Maintaining a constant-mode profile across the entire waveguide (i.e., from the incoupling prism to the outcoupling grating) requires that the prism–waveguide gap be filled with solution.<sup>31,32</sup>

- (14) Dunphy, D. R.; Mendes, S. B.; Saavedra, S. S.; Armstrong, N. R. *Anal. Chem.* **1997**, *69*, 3086–3094.
- (15) Dunphy, D. R.; Mendes, S. B.; Saavedra, S. S.; Armstrong, N. R. In *Interfacial Electrochemistry*; Wieckowski, A., Ed.; Marcel Dekker: New York, 1999; pp 513–525.
- (16) Kogelnik, H. In *Integrated Optics*; Tamir, T., Ed.; Springer-Verlag: New York, 1979; Vol. 7, pp 13–81.
- (17) Plowman, T. E.; Saavedra, S. S.; Reichert, W. M. *Biomaterials* **1998**, *19*, 341–355.
- (18) Midwinter, J. E. *IEEE J. Quantum Electron.* **1971**, *QE-7*, 345–350.
- (19) Hammer, J. M. U.S. patent 4,152,045, May 1, 1979; p 4.
- (20) Spaulding, K. E.; Morris, G. M. *Appl. Opt.* **1991**, *30*, 1096–1112.
- (21) Spaulding, K. E.; Morris, G. M. *J. Lightwave Technol.* **1992**, *10*, 1513–1518.
- (22) Hetherington, D. L.; Kostuk, R. K.; Gupta, M. C. *Appl. Opt.* **1993**, *32*, 303–308.
- (23) Strasser, T. A.; Gupta, M. C. *Appl. Opt.* **1994**, *33*, 3220–3226.
- (24) Li, L.; Brazas, J. C. J. U.S. patent 5,420,947, May 5, 1995; p 12.
- (25) Mendes, S. B.; Li, L.; Burke, J. J.; Lee, J. E.; Saavedra, S. S. *Appl. Opt.* **1995**, *34*, 6180–6186.
- (26) Mendes, S. B.; Li, L.; Burke, J. J.; Lee, J. E.; Dunphy, D. R.; Saavedra, S. S. *Langmuir* **1996**, *12*, 3374–3376.
- (27) Mendes, S. B.; Li, L.; Burke, J. J.; Saavedra, S. S. *Opt. Commun.* **1997**, *136*, 320–326.
- (28) Bradshaw, J. T.; Mendes, S. B.; Saavedra, S. S. *Anal. Chem.* **2002**, *74*, 1751–1759.

- (29) Li, L.; Xu, M.; Stegeman, G. I.; Seaton, C. T. *Proc. SPIE-Int. Soc. Opt. Eng.* **1987**, *835*, 72–82.
- (30) Brazas, J. C.; Li, L. *Appl. Opt.* **1995**, *34*, 3786–3792.
- (31) Saavedra, S. S.; Reichert, W. M. *Appl. Spectrosc.* **1990**, *44*, 1210–1217.
- (32) Saavedra, S. S.; Reichert, W. M. *Appl. Spectrosc.* **1990**, *44*, 1420–1423.

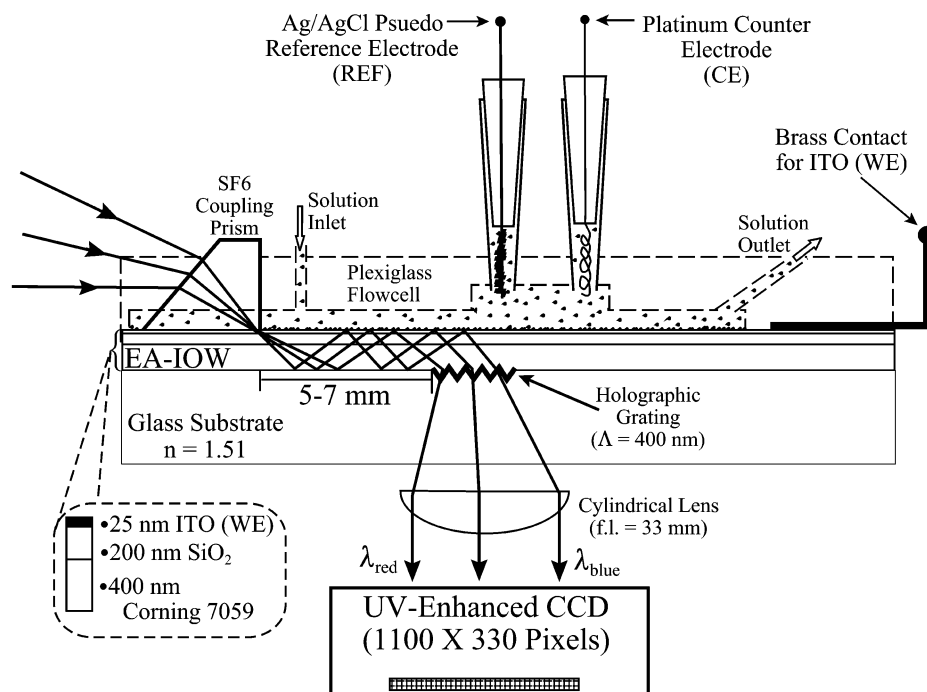


Figure 1. Device schematic of the broadband EA-IOW spectrometer. Light is focused into the SF6 prism, coupled into the multilayer EA-IOW, guided along its long axis via total internal reflection, and outcoupled through the glass substrate by a surface relief grating (grating period 400 nm). The outcoupled light is collimated with a 33-mm focal length (f.l.) cylindrical lens onto a CCD camera. Incoupler to outcoupler distance for experiments reported herein ranged from 5 to 7 mm. Two electrode ports accommodate reference and counter electrodes, while a thin piece of brass sheeting acts as a contact to the thin ITO working electrode. Note: EA-IOW layer thicknesses are not drawn to scale.

The optical layout for all experiments was identical to the layout previously described,<sup>28</sup> except that a mirror was used in place of the long-pass dichroic filter (see Figure 1b in ref 28). To minimize stray light, the entire rotary stage was placed inside a light-tight enclosure, and the entire back surface of the waveguide was coated with a black strippable paint (X-59 Strip Coating, Universal Photonics), except for a small window over the outcoupling grating. Use of the black paint also aided in the suppression of spurious substrate modes.

Silicon sheeting was used as the gasket material in the spectroelectrochemical flow cell (Figure 1), providing an active electrode area of  $\sim 7.5$  cm<sup>2</sup>. Reference and counter electrodes were mounted directly opposite the critical electroactive region of the waveguide (as shown in Figure 1). The reference electrode was fabricated by switching potentials between a silver wire and a platinum wire immersed in a saturated KCl solution, using a 9-V battery as a power supply. Since the anodized silver wire was immersed directly into the analyte solution, rather than maintained in a solution of fixed electrolyte concentration, it represents a "pseudo" Ag/AgCl reference electrode. It was periodically remade and calibrated against the Fe(CN)<sub>6</sub><sup>3-</sup>/Fe(CN)<sub>6</sub><sup>4-</sup> redox couple. The counter electrode was a coiled platinum wire. The EA-IOW potential was controlled using an EG&G potentiostat (Princeton Applied Research, model 263A).

**Broadband EA-IOW Spectrometer Characterization.** Prior to any experimentation, waveguides were cleaned as follows: (a) sonication (20–30 min) in absolute ethanol (200 proof, AAPER Alcohol); (b) light scrubbing with cotton soaked in a 1% Liqui-Nox solution; (c) sonication in 1% Liqui-Nox solution; (d) rinsing, sonication, and rinsing again in deionized water (Barnstead

Nanopure system, resistivity 18 M $\Omega$ ·cm, total organic content <10 ppb). Cleaned waveguides were stored in a solution of supporting electrolyte (5 mM sodium phosphate in deionized water, pH 7, unless specified otherwise) for a period of at least 24 h.

Various experiments were performed to characterize the broadband response of the EA-IOW. Initially, broadband coupling was visually verified (vide infra) with the flow cell filled with supporting electrolyte solution without controlling the applied potential. As performed with the previously described sol-gel planar IOW spectrometer,<sup>28</sup> upon achieving broadband coupling, the peak throughput of several narrow band-pass filters was used for alignment and wavelength calibration of the CCD camera. Collinear alignment of various laser sources with the optical axis of the broadband source (150-W xenon arc lamp) allowed for assessment of spectral resolution. Image integration times were determined by measuring CCD response at successively longer exposure times, with  $\sim 80\%$  of the full well capacity used for the integration time in all experiments. All spectra consisted of at least three summed acquisitions.

Band-pass filter throughput was also measured with the EA-IOW under potential control versus a pseudo Ag/AgCl reference electrode. Prior to any spectral measurements, the flow cell was filled with supporting electrolyte solution and the EA-IOW was electrochemically equilibrated by cycling the applied potential at least 20 times at 200 mV/s between +400 and -400 mV, followed by 20 times at 100 mV/s, and finally 10 times at 20 mV/s. Previous work has shown that electrochemical equilibration with electrolyte is crucial for suppression of hysteresis in the optical background.<sup>14,15,33</sup> After equilibration, the ITO was scanned to the

desired potential and held for several minutes until the measured current reached an apparent plateau, at which point spectral measurements commenced.

Waveguide incoupling profiles (i.e., intensity of light outcoupled from the EA-IOW as a function of the incident angle of the source beam on the coupling prism) were measured for various laser lines as a function of applied potential. The rotary stage was translated incrementally through an arc of  $\sim 3^\circ$ , and the outcoupled intensity was measured with a laser power meter (Metrologic 45–540) at  $\sim 15$  positions within the angular range.

**Protein Adsorption Protocol.** EA-IOWs were cleaned as described above. With the flow cell filled with supporting electrolyte solution and without controlling the applied potential, raw throughput intensities (i.e., flatfield spectra) for both TE and TM polarizations were measured as a function of incoupling angle (over an  $\sim 3^\circ$  range centered about the initial coupling angle) in order to maximize throughput in the 500–550-nm region, which is the region in which the  $\alpha$  and  $\beta$  absorbance bands of horse heart cytochrome *c* occur. Electrochemical equilibration was performed and flatfield spectra were collected at  $-400$  and  $+400$  mV. Background cyclic voltammograms were collected at scan rates of 20 and 100 mV/s. Without controlling the applied potential, 35  $\mu\text{M}$  horse heart ferricytochrome *c* (ferricyt *c*, 99%, Sigma), freshly purified by separation on a carboxymethyl cellulose column (CM-52, Whatman),<sup>34</sup> was then injected into the flow cell and incubated at room temperature for 30 min. Previous experience has shown that this results in adsorption of  $\sim 30\%$ <sup>35</sup> of a theoretically full packed monolayer<sup>36</sup> on an EA-IOW surface. The potential of the EA-IOW surface was then scanned (20 mV/s) from rest potential to  $-400$  mV and held for  $\sim 2$  min, at which point the ATR spectrum was collected. The potential was then scanned to  $+400$  mV, held for  $\sim 2$  min, and an ATR spectrum was again collected. Cyclic voltammograms at sweep rates of 20 and 100 mV/s were collected without flushing the flow cell. The flow cell was then flushed with supporting electrolyte solution, and the potential scanning procedure was repeated, with ATR spectra collected at  $-400$  and  $+400$  mV.

**Adsorption Protocol for Ferrocenedicarboxylic Acid.** 1,1'-Ferrocenedicarboxylic acid ( $\text{Fc}(\text{COOH})_2$ , Aldrich) was adsorbed to EA-IOW surfaces from ethanol. EA-IOWs were cleaned as described above, supplemented with a final sonication step in ethanol, followed by incubation in supporting electrolyte solution (0.1 M  $\text{LiClO}_4/\text{ethanol}$ ) for  $\sim 24$  h. Waveguide coupling was achieved and optimized in the same manner as described for the cyt *c* experiments, followed by the electrochemical equilibration steps and collection of flatfield spectra. The potential window was 0.0 V to  $+1.40$  V. Background cyclic voltammograms were collected at scan rates of 20 and 100 mV/s. A 100  $\mu\text{M}$   $\text{Fc}(\text{COOH})_2$  solution was then injected into the flow cell and incubated at room temperature for 10 min. The spectroelectrochemical response was measured in the same manner as in the cyt *c* experiment. The system was flushed with supporting electrolyte and the spectral

response to the potential end points was measured again. Timed acquisition spectra were also collected by synchronous spectral collection during a slow voltammetric sweep (20 mV/s).

## RESULTS AND DISCUSSION

**Broadband Coupling Approach.** Mendes et al.<sup>25–27</sup> described two different approaches for achieving achromatic coupling into a single-mode, planar glass IOW. In the first approach, the optical parameters of a given IOW were characterized and a multi-component incoupling element that “matched” that IOW was fabricated. In the second approach, the optical parameters were “matched” for a given IOW and a commercially available glass material (from which a single prism incoupler was made). In theory, this second approach could also be implemented by “tailoring” the optical parameters of a waveguide layer to match the parameters of a commercially available glass prism. The second approach was technically much simpler (i.e., a single prism versus a prism/multiple grating combination). However, the optical parameters of the EA-IOW are not “matched” by any commercial glass, and altering the optical parameters of the EA-IOW was not deemed feasible, given that a significant amount of “tailoring” was required to develop the monochromatic version of this device.<sup>14,15</sup> Hence, the first approach was pursued initially in an effort to create a broadband-coupled EA-IOW. The optical dispersion of the EA-IOW was measured, and theoretical design of an achromatic incoupling element was initiated. However, prior to significant progress toward this design, we developed a much simpler approach to broadband coupling.<sup>28</sup>

Although this simpler approach was developed for a sol–gel glass, planar IOW, it was also found to result in broadband coupling when applied to the EA-IOW. As shown in Figure 1, a single prism is clamped to the surface of the EA-IOW and an incident beam with a relatively large numerical aperture (NA) is focused onto the hypotenuse face. Using a large NA produces numerous angles of incidence for *all* wavelengths from a broadband source. Assuming the NA is large enough, an incident angle that produces a resonant waveguide mode should exist for each wavelength within a broad spectral range. At all incidence angles that do not correspond to resonant mode excitation, each wavelength will be rejected (i.e., reflected; see Figure 2 of ref 28 for a more complete description of this process). The principle issue with this simpler approach is not *if* multiple wavelengths can be simultaneously incoupled, but *how much* energy from each wavelength can be incoupled, versus the amount rejected by off-angle incidence. As described below, sufficient light can be coupled into the EA-IOW to make it a viable tool for performing broadband IOW-ATR spectroscopy of electrochemically active molecular films.

The general procedure followed in developing a broadband EA-IOW-ATR spectrometer was very similar to that previously described for the sol–gel glass-based IOW-ATR spectrometer.<sup>28</sup> Broadband coupling using the “all lines” mode of an argon ion laser (Coherent, I70-5) was first attempted. Several  $\text{Ar}^+$  lines (514.5, 501.7, 496.5, 488.0, and 476.5 nm) were focused into the incoupling prism (at a single incident angle), observed to guide along the length of the EA-IOW, then outcoupled and spatially dispersed at the diffraction grating. Incoupling white light from a 150-W xenon arc lamp was also visually confirmed; outcoupling was observed for most of the visible spectrum, with the violet

(33) Doherty, W. J., III; Donley, C.; Armstrong, N. R.; Saavedra, S. S. *Appl. Spectrosc.* **2002**, *56*, 920–927.

(34) Brautigan, D. L.; Ferguson-Miller, S.; Margoliash, E. In *Methods in Enzymology*; Academic Press: New York, 1978; Vol. 53D, pp 128–164.

(35) Robertson, R. T. Ph.D. Dissertation, University of Arizona, Tucson, AZ, 2001.

(36) Edmiston, P. L.; Lee, J. E.; Cheng, S.-S.; Saavedra, S. S. *J. Am. Chem. Soc.* **1997**, *119*, 560–570.

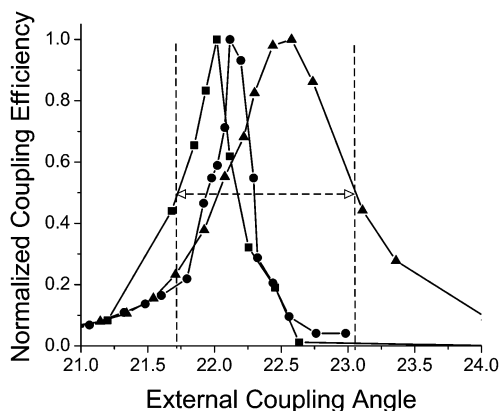


Figure 2. Normalized outcoupling intensity profiles for laser lines 514.5 (■), 543.4 (●), and 632.8 nm (▲), measured as a function of incident beam coupling angle, for the broadband coupled EA-IOW. Individual curves were normalized to their respective maximum intensity. These profiles were measured with no potential applied to the EA-IOW. The dashed lines indicate the half-maximum intensity of the 514.5- and 632.8-nm profiles and are shown as a representation of the approximate incident beam NA that would be required to achieve simultaneous incoupling of all three laser lines.

end of the spectrum noticeably absent, which is attributed to absorbance by the ITO layer.

When a broadband lamp is used as a source for waveguide spectroscopy, it is difficult to visually distinguish between light propagating in a resonant waveguide mode from light propagating in a substrate mode due to the large spot size, low intensity for individual wavelengths, and poor degree of collimation (which are characteristics of an incoherent source relative to a laser source). Two procedures<sup>28</sup> were utilized to verify that light outcoupled at the diffraction grating originated from white light propagating in the waveguide modes of the EA-IOW, rather than in the substrate modes that extend across the entire thickness of both the EA-IOW and the microscope slide substrate. First, laser lines were coupled into the waveguide simultaneously with the white light source. When a 5.0-mW HeNe laser (543.4 nm), a 30-mW HeNe laser (632.8 nm), and a 6-W Ar<sup>+</sup> laser (in the “all lines” mode) were collinearly aligned with the xenon arc lamp, all sources were visually observed to produce a waveguide “streak” along the EA-IOW length at approximately the same incident angle, showing that the outcoupled, dispersed white light was most likely coming from a propagated waveguide mode. Second, a small spot of black ink was applied to the waveguide surface. If the white light was guiding in a resonant mode, it would propagate until it encountered the black spot, at which point it was extinguished. In contrast, the black ink had a negligible effect on white light propagating in a substrate mode, simply due to the much smaller evanescent path length.

Waveguide incoupling profiles measured for laser lines at 514.5, 543.4, and 632.8 nm are shown in Figure 2. The profiles overlapped significantly, which is attributed to the dispersion in incident angles. A conservative estimate of the NA of the incident beam required to achieve simultaneous coupling of all three lines can be obtained from the dashed line plotted in Figure 2. The angular width defined by this dashed line is 1.32°, which can be achieved using an incident beam with a NA of 0.012. The data also show that, at an incident angle of ~22.1°, all three laser lines were

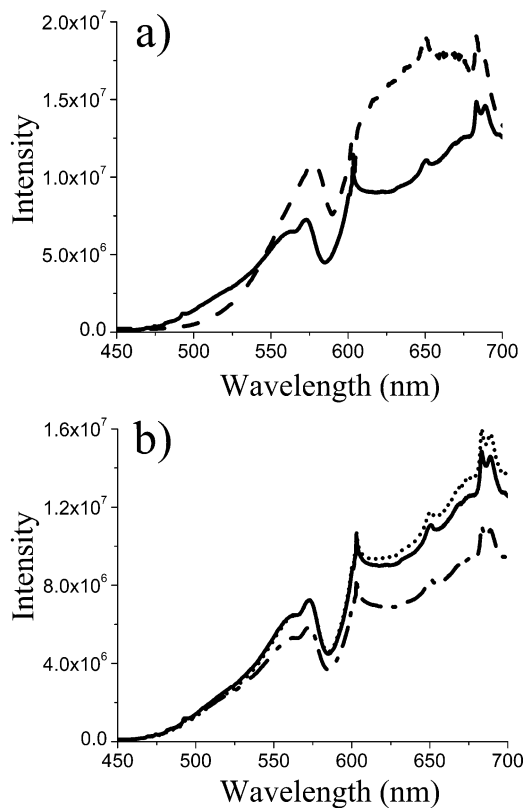


Figure 3. (a) Flatfield spectral throughput of the broadband EA-IOW spectrometer for TE (---) and TM (—) polarizations. (b) Potential-dependent throughput for TM polarized light at 0 (—), -400 (— · —), and +400 mV (···). Intensity values are plotted in arbitrary units registered by the CCD camera. These spectra were collected using a flow cell filled with aqueous buffer; spectra collected with ethanol in the flow cell were very similar. A 150-W Xe arc lamp was used as the source.

incoupled at >60% of their maximum coupling efficiency due to the angular overlap.<sup>37</sup>

Flatfield spectra (i.e., raw throughput intensities), collected at open potential in the TE<sub>0</sub> and TM<sub>0</sub> modes, are shown in Figure 3a. The incident angle was adjusted in order to maximize throughput in the 500-nm region. Adjusting the incident angle had a greater effect on throughput of wavelengths of <580 nm, whereas for wavelengths of >580 nm, throughput varied little over an incoupling angular range of ~3°. It should be noted that spectral throughput is dependent on the particular waveguide used and on coupling conditions (e.g., coupling angle, intimacy of prism/waveguide contact, position, and optical properties of the incident beam). However, the variability among individual EA-IOWs was found to be significantly less than that observed for sol-gel planar IOWs.<sup>28</sup> Ten separate spectroelectrochemical experiments were performed using five different EA-IOWs; the optimum incident coupling angle for throughput in the 500–550-nm region ranged from 22.2° to 22.7° ( $\bar{x} = 22.4^\circ$ ,  $S_d = 0.16^\circ$ ). This small variability, relative to the much greater variability of sol-gel derived IOWs,<sup>28</sup> is attributed to the more reproducible nature of vacuum deposition methods used to produce EA-IOWs.

(37) This estimate is for incidence precisely at 22.1° (i.e., NA = 0); the efficiency should therefore be greater when the NA of the incident beam is taken into consideration.

Table 1. Comparison of Filter Spectra Collected with the EA-IOW and a Conventional, Transmission-Based Spectrometer

		band-pass filter <sup>a</sup>			
		500 nm	550 nm	633 nm	700 nm
EA-IOW	peak abs (% <i>T</i> )	23.6	48.6	63.6	8.9
	$\lambda_{\max}^b$ (nm)	501.2	545.8	636.4	700.0
	fwhm <sup>c</sup> (nm)	9.0	9.7	10.3	10.8
conventional spectrometer	peak abs (% <i>T</i> )	27.2	50.4	65.4	11.1
	$\lambda_{\max}$ (nm)	500.0	545.6	636.7	700.1
	fwhm (nm)	9.7	9.6	10.4	11.1

<sup>a</sup> Filter wavelengths are nominal. <sup>b</sup> Measured center wavelength of filter. <sup>c</sup> Full width at half-maximum.

Spectral throughput of the EA-IOW has also been shown to be strongly dependent upon incident beam polarization.<sup>15</sup> Numerical modeling of the optical properties of the EA-IOW, based on solutions to Maxwell's equations, produces calculated mode profiles (i.e., electric field intensity as a function of distance along the axis normal to the waveguide plane), showing that a much higher percentage of the total light is guided in the ITO layer in the TE<sub>0</sub> mode relative to the TM<sub>0</sub> mode.<sup>15</sup> This produces a 4-fold sensitivity enhancement in TE<sub>0</sub> versus TM<sub>0</sub> but also a higher propagation loss. The practical result is that the TE<sub>0</sub> mode, while more sensitive, exhibits a much lower total throughput than the TM<sub>0</sub> mode. Furthermore, measurements in TE<sub>0</sub> are more subject to interference by stray light. As a consequence, the TE<sub>0</sub> response shown in Figure 3a required a 350-ms acquisition time, whereas the TM<sub>0</sub> response was acquired in only 75 ms.

The spectral performance of the broadband EA-IOW spectrometer was compared to that of a conventional UV-visible instrument (Spectral Instruments, model 440) by measuring transmission spectra of band-pass filters on both instruments. For the EA-IOW spectrometer, the filters were placed in the beam path and the ratio of the intensity propagated through the optical train (*I*) to the background flatfield spectrum (i.e., spectrum with no filter in the beam path, *I*<sub>0</sub>) was determined. Table 1 presents a comparison of spectra of four filters that span ~200 nm of the visible spectrum, showing that the EA-IOW spectrometer produced spectral profiles nearly identical to those obtained from the conventional spectrometer. A small difference in EA-IOW response, on the blue side of the 500-nm filter spectrum (see Supporting Information for a graphical comparison), indicates the onset of limited throughput in the blue spectral region due to the optical loss associated with the 25-nm ITO layer. The limited throughput in turn caused systematic errors in this spectral region due to the greater influence of stray light (vide infra). The spectral comparison also shows that the bandwidth of the EA-IOW spectrometer extends from ~495 to ~705 nm. This 210-nm bandwidth is comparable to that observed for the broadband sol-gel IOW spectrometer.<sup>28</sup>

Spectral resolution was assessed by measuring the peak widths at half-maximum for multiple Ar<sup>+</sup> and HeNe laser lines. The measured fwhm for three of the Ar<sup>+</sup> laser lines was: 0.70 nm for the 496.5- and 514.5-nm lines and 0.63 nm for the 501.7-nm line. Fwhm values for the HeNe lines were 0.74 and 0.84 nm for the 543.4- and 632.8-nm lines, respectively. This range in fwhm values (0.63–0.84 nm) is smaller than the ranges reported for both the

broadband sol-gel IOW spectrometer (0.5–1.3 nm) and for the conventional UV-visible spectrometer (1.5–2.4 nm).<sup>28</sup> Thus, the resolving power of the broadband EA-IOW spectrometer is comparable to that of a commercial transmission instrument, demonstrating its adequacy for measuring and resolving molecular absorbance bands in the visible region.

**Potential-Dependent Waveguide Performance.** The waveguide incoupling profiles shown in Figure 2 were measured without application of a potential to the EA-IOW. Results from previous studies suggested that the guiding characteristics of the waveguide might change significantly as the potential was scanned, which could make it difficult to simultaneously couple multiple wavelengths into the waveguide.<sup>14,15</sup> Thus, incoupling profiles were also measured at applied potentials of 0, -400, and +400 mV (data not shown). There were minor differences between these profiles and those plotted in Figure 2. As a quantitative comparison, the region defined by the dashed lines in Figure 2 ranged from an angular width of 1.32° (at no applied potential) to 1.71° (at 0 mV); the angular widths at -400 and +400 mV fell between these values. The midpoint of the dashed line region deviated from the no applied potential case by a maximum of 0.34° (at -400 mV). Hence, the incoupling profiles changed very little over a potential window of 800 mV. Over this window, an incident beam with a NA of only 0.015 would be required to achieve broadband coupling from 514.5 to 632.8 nm.

In contrast, Figure 3b shows that the flatfield spectrum is dependent on applied potential and that the dependence is more pronounced at wavelengths of >550 nm. These data are consistent with previous observations.<sup>15</sup> Since the throughput changes with applied potential, background flatfield spectra (*I*<sub>0</sub>) must be collected at a variety of applied potentials in order to calculate absorbance values at those potentials (vide infra).

The optical properties of the ITO layer are described by its complex refractive index (*n*\*), given by  $n^* = n - ik$ , where *n* is the real refractive index and *k* is the imaginary component that defines the extinction coefficient of the material. ITO is highly transparent over most of the visible spectrum due to the predominance of a relatively flat *n* value coupled with a negligible *k* value. This transparency diminishes at wavelengths of <500 nm due to a sharp increase in *k* caused by proximity to the band-edge absorption.<sup>15,38,39</sup> Since the crystal structure of ITO is complex (and only partially understood), the band-edge absorption is not a discrete transition but extends over a spectral region extending from the ultraviolet to ~400–450 nm. These optical transparency changes are also dependent on free carrier concentration in this nearly degenerate semiconductor and on the applied potential.<sup>39</sup> Therefore, changes in free carrier density that result from the respective changes in applied potential are a probable explanation for the differences in the flatfield spectra plotted in Figure 3b.

The effective refractive index of a waveguide (*N*<sub>wg</sub>), defined as the projection of the wave vector onto the waveguide plane, is a function dependent on the respective *n*\* and thickness (*t*) of each layer in the waveguide, the indices of refraction of the substrate (*n*<sub>s</sub>\*) and cover layers (*n*<sub>c</sub>\*), and the wavelength of light ( $\lambda$ ).<sup>25</sup> The effective index can be separated into real and imaginary components ( $N_{wg} = N_R - iN_I$ ). *N*<sub>I</sub> is composed of the absorptivities

(38) Dunphy, D. R. Ph.D. Dissertation, University of Arizona, Tucson, AZ, 1998.

(39) Hartmagel, H. L.; Dawar, A. L.; Jain, A. K.; Jagadish, C. *Semiconducting Transparent Thin Films*; Institute of Physics Publishing: Bristol, 1995.

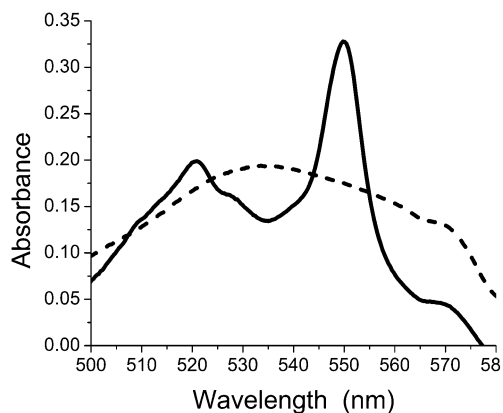


Figure 4. ATR spectra of a submonolayer of cytochrome *c* adsorbed to the surface of the EA-IOW. The spectra were collected in the following order: (i) electrochemically reduced ferrocytochrome *c* (—), after scanning the potential from 0 to  $-400$  mV and holding at  $-400$  mV for  $\sim 2$  min, (ii) after scanning the potential to  $+400$  mV to produce ferricytochrome *c* (---). Each spectrum was referenced to a phosphate buffer blank collected at the respective potential endpoint (i.e.,  $-400$  and  $+400$  mV).

of all the waveguide layers; thus  $N_{wg}$  is complex when at least one layer absorbs light, which is the case for the ITO layer in the EA-IOW. The relation between the ITO band gap energy and the number of free carriers predicts that  $N_i$  should be dependent on applied potential.

To further explore the effect of applied potential on the guiding characteristics of the EA-IOW, transmission spectra of a narrow band-pass filter centered at  $514$  nm were measured at  $0$  V,  $-400$  mV, and  $+400$  mV. Minimal differences among these spectra were observed (data not shown, see Supporting Information). Thus, despite the predicted dependence of  $N_i$  on applied potential,  $N_{wg}$  appears to be relatively unaffected over an  $800$ -mV potential window. Consequently, the changes in outcoupled intensity shown in Figure 3b can be entirely attributed to waveguide loss caused by the band gap absorptivity of the ITO layer and not due to a “detuning” of the coupling angle caused by a change in  $N_{wg}$ .

**Protein Adsorption Experiments.** Horse heart cytochrome *c* was chosen as a test sample for assessing the capabilities of the broadband EA-IOW spectrometer for measuring ATR spectra of a redox-active submonolayer film for the following reasons: (a) the electrochemistry of cytochrome *c* adsorbed to electrode surfaces, including ITO, has been studied extensively;<sup>40–45</sup> (b) the absorbance spectra of ferricytochrome *c* and ferrocytochrome *c* are easily distinguishable in the  $500$ – $600$ -nm spectral region;<sup>46</sup> and (c) at dissolved concentrations of  $> 10$   $\mu$ M, the protein adsorbs very strongly to ITO, producing  $\sim 30\%$  of a theoretical close packed monolayer.<sup>35</sup>

Figure 4 displays the EA-IOW-ATR spectral response of an adsorbed layer of cytochrome *c* at potentials necessary to keep the protein either in its fully reduced (i.e., scan to  $-0.400$  V vs Ag/AgCl, hold

for 2 min) or in its fully oxidized state (i.e.,  $+0.400$  V vs Ag/AgCl). Reduction of the cytochrome *c* layer caused a blue shift of the  $\beta$  band and the appearance of the  $\alpha$  band, consistent with expectations based on the spectral properties of native (dissolved) cytochrome *c* and other related hemoproteins.<sup>46–50</sup> Reoxidization caused a red shift of the  $\beta$  band and the disappearance of the  $\alpha$  band.

It is significant to note that these spectra were acquired in the  $TM_0$  mode and that the entire spectral range from  $500$  to  $\sim 600$  nm was interrogated simultaneously. Although not shown here, spectra of this sample could also be acquired readily in the  $TE_0$  mode. Thus, the EA-IOW spectrometer can be used to measure broadband dichroic ATR spectra, which makes this technology a useful research tool for studying molecular orientation in thin films.<sup>36</sup>

It is useful to compare the sensitivity of the broadband EA-IOW technology to a conventional transmission geometry. By combining path length  $b$  with concentration  $C$ , which gives surface coverage  $\sigma$ , and recasting  $\epsilon$  in units of  $\text{cm}^2/\text{mol}$ , the standard Beer's law expression ( $A = \epsilon b C$ ) can be used to calculate the absorbance of a cytochrome *c* film measured in transmission geometry. For a ferrocytochrome *c* film with a surface coverage of  $6.6 \times 10^{-12}$  mol/ $\text{cm}^2$ , the calculated absorbance is  $1.83 \times 10^{-4}$  AU, assuming  $\epsilon_{550.25 \text{ nm}} = 27\,700 \text{ M}^{-1} \text{ cm}^{-1}$ . Thus, the EA-IOW-ATR spectrometer provides a sensitivity enhancement of  $\sim 1800$  relative to a transmission geometry. This enhancement agrees well with previously reported results.<sup>14,15</sup>

**Spectroelectrochemical Characterization of Adsorbed  $\text{Fc}(\text{COOH})_2$ .** To assess the sensitivity of the EA-IOW, experiments were also performed using a chromophore,  $\text{Fc}(\text{COOH})_2$ , having a significantly lower molar absorptivity ( $\epsilon$ ) than cytochrome *c*. For both the oxidized and reduced forms of ferrocenes,  $\epsilon$  values are typically  $500$ – $1000 \text{ M}^{-1} \text{ cm}^{-1}$ .<sup>51</sup> Substituted ferrocenes adsorb to ITO from polar organic solvents (e.g., ethanol) and undergo reversible oxidation/reduction in the adsorbed state.<sup>52</sup> We have recently shown that voltammetry of adsorbed  $\text{Fc}(\text{COOH})_2$  can be used to monitor changes in surface composition of ITO electrodes, as a function of different chemical and physical cleaning steps prior to immersion into the electrolyte.<sup>53</sup> Adsorption may occur through hydrogen bonding of the carboxylic acid groups to the hydroxide sites on the ITO surface, through coordination of these carboxylic acid groups with metal cation defect sites in the near-surface region, or through both. For all types of electrode surface pretreatment, we found that a maximum of  $\sim 40$ – $50\%$  of a close-packed monolayer of  $\text{Fc}(\text{COOH})_2$  was electrochemically active (i.e., a considerable fraction of the adsorbed monolayer is redox inactive).

Prior to this work, all EA-IOW experiments had been carried out in aqueous solutions.<sup>14,15,35,38</sup> Hence, the performance characteristics of the EA-IOW in ethanol were untested. Therefore, prior to studying the behavior of adsorbed  $\text{Fc}(\text{COOH})_2$ , all of the

(40) Hawkrige, F. M.; Taniguchi, I. *Comments Inorg. Chem.* **1995**, *17*, 163–187.

(41) Willit, J. L.; Bowden, E. *J. Phys. Chem.* **1990**, *94*, 8241–8246.

(42) Collinson, M.; Bowden, E. F. *Anal. Chem.* **1992**, *64*, 1470–1476.

(43) Song, S.; Clark, R. A.; Bowden, E. F.; Tarlov, M. *J. Phys. Chem.* **1993**, *97*, 6564–6572.

(44) Kasmi, A. E.; Wallace, J. M.; Bowden, E. F.; Binet, S. M.; Linderman, R. J. *J. Am. Chem. Soc.* **1998**, *120*, 225–226.

(45) Kasmi, A. E.; Leopold, M. C.; Galligan, R.; Robertson, R. T.; Saavedra, S. S.; Kacemi, K. E.; Bowden, E. F. *Electrochem. Commun.* **2002**, *4*, 177–181.

(46) Margoliash, E.; Frohwirt, N. *Biochem. J.* **1959**, *71*, 570–572.

(47) Estabrook, R. W. *J. Biol. Chem.* **1957**, *223*, 781–794.

(48) Eaton, W. A.; Hochstrasser, R. M. *J. Chem. Phys.* **1967**, *46*, 2533–2539.

(49) Owens, J. W.; O'Connor, C. *J. Inorg. Chim. Acta* **1988**, *151*, 107–116.

(50) Coletta, M.; Costa, H.; De Sanctis, G.; Neri, F.; Smulevich, G.; Turner, D. L.; Santos, H. *J. Biol. Chem.* **1997**, *272*, 24800–24804.

(51) Rulkens, R.; Lough, A. J.; Manners, I.; Lovelace, S. R.; Grant, C.; Geiger, W. E. *J. Am. Chem. Soc.* **1996**, *118*, 12683–12695.

(52) Zotti, G.; Schiavon, G.; Zecchin, S.; Berlin, A.; Pagani, G. *Langmuir* **1998**, *14*, 1728–1733.

(53) Donley, C.; Dunphy, D.; Paine, D.; Carter, C.; Nebesny, K.; Lee, P.; Alloway, D.; Armstrong, N. R. *Langmuir* **2001**, *18*, 450–457.

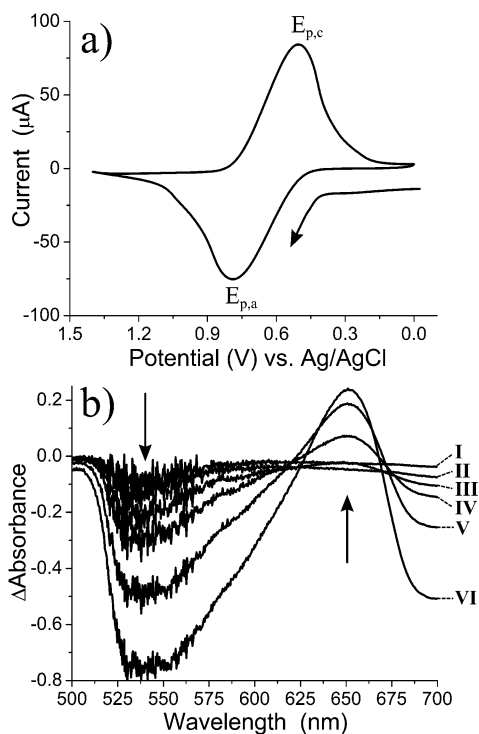


Figure 5. Voltammetry and EA-IOW-ATR spectroscopy of an adsorbed  $\text{Fc}(\text{COOH})_2$  film. (a) Cyclic voltammogram collected by scanning between 0.0 and +1.40 V versus Ag/AgCl. Scan rate 20 mV/s. (b) EA-IOW-ATR difference spectra measured at applied potentials of (I) 200, (II) 400, (III) 600, (IV) 700, (V) 800, and (VI) 900 mV. The arrows indicate the direction of change for the spectral bands observed.

waveguide performance characterization procedures described above (i.e., broadband coupling with laser and Xe sources, spectral comparison using band-pass filters, assessment of spectral resolution, characterization of potential-dependent waveguiding, etc.) were performed with the flow cell filled with 0.1 M  $\text{LiClO}_4/\text{ethanol}$ . In general, the waveguiding properties of the EA-IOW were observed to be superior (e.g., incoupling was much easier to accomplish, the waveguide streak was better defined visually, and outcoupling was visibly more intense) than when the flow cell was filled with water or aqueous buffer. The spectral performance with the flow cell filled with ethanol was also equal to or slightly better than the performance in buffer, as evidenced by a comparison of band-pass filter spectra (data not shown) and fwhm values of 0.75 and 0.68 nm for the 543.4- and 632.8-nm HeNe laser lines, respectively (vide supra).

A 100  $\mu\text{M}$  solution of  $\text{Fc}(\text{COOH})_2$  was equilibrated with the EA-IOW, followed by a rinse of the flow cell with supporting electrolyte solution, followed by voltammetric characterization of the remaining adsorbed material. A typical voltammetric response is shown in Figure 5a. The surface coverage of  $\text{Fc}(\text{COOH})_2$ , estimated to be  $\sim 1.7 \times 10^{-9}$  mol/cm<sup>2</sup> by integration of the voltammogram, was equivalent to adsorption of about four monolayers. Since the rms surface roughness of the EA-IOW is  $\sim 0.9$  nm (from atomic force imaging on a  $\sim 1 \mu\text{m}^2$  area),<sup>38</sup> it is likely that H-bonding between  $\text{Fc}(\text{COOH})_2$  layers is responsible for multilayer adsorption (i.e., the first monolayer is adsorbed through one carboxy group per molecule, leaving an exposed carboxy group available for interaction with a dissolved

$\text{Fc}(\text{COOH})_2$  molecule). After multilayer adsorption, extensive flushing of the flow cell multiple times with supporting electrolyte solution generated little observable change in voltammetric response, showing that desorption did not occur. However,  $\text{Fc}(\text{COOH})_2$  was completely desorbed, at all surface coverages, by flushing the flow cell with aqueous buffer.

Differential EA-IOW-ATR spectra of  $\text{Fc}(\text{COOH})_2$  multilayer films, collected at various potentials during a voltammetric scan, are plotted in Figure 5b. Oxidation of the  $\text{Fc}(\text{COOH})_2$  film caused the absorbance to decrease in the wavelength region below 575 nm, accompanied by growth of a new absorbance band with a  $\lambda_{\text{max}}$  near 645 nm, which is the ligand-to-metal charge-transfer band of the ferricenium cation.<sup>51</sup> The decreased absorbance at  $< 575$  nm, relative to neutral ferrocene, should actually be observed as a band with a  $\lambda_{\text{max}}$  near 450 nm,<sup>51</sup> but the limited transparency of the EA-IOW below 525 nm only allowed a shoulder from that band to be observed. Well-defined isosbestic points near 620 and 670 nm were expected in the difference spectra presented in Figure 5b. Although present, they were not well resolved. This is attributed to shifts in the optical background, caused by environmental drift, including the changing potential of the ITO layer (see refs 14, 15, and 38). This problem could be minimized by implementing a dual-beam instrumental arrangement, although this would be a significant engineering challenge.

## CONCLUSIONS

Application of a simplified broadband coupling approach to the single-mode, step index, EA-IOW has been employed to create a broadband, electroactive planar waveguide spectrometer. The optical performance of this spectrometer compares well with that of a commercially available, transmission-based instrument and with the recently reported broadband sol-gel planar IOW-ATR spectrometer.<sup>28</sup> The capability of this device to measure broadband ATR spectra of thin molecular films over a visible wavelength range from about 500 to 700 nm, coupled with the capability to electrochemically modulate the redox state of the adsorbed film, makes the EA-IOW spectrometer a multidimensional measurement tool with an unprecedented combination of sensitivity and spectral information content. Application of a surface-confined molecular recognition layer would further improve the multidimensional features, with potential applications in chemical sensing.<sup>13,54–56</sup> Furthermore, since light propagating in the EA-IOW is polarized (in either  $\text{TE}_0$  or  $\text{TM}_0$ ), this technology should allow the molecular orientation of adsorbed molecules to be characterized as a function of redox state.<sup>36</sup>

## ACKNOWLEDGMENT

This material is based upon work partially supported by the National Institutes of Health under Grant R21GM59242 (to S.S.S. and N.R.A.) and by the National Science Foundation under Grants CHE-0108805 to S.S.S. and CHE-9732650 to N.R.A. J.T.B. gratefully acknowledges Anne Runge for assisting in the purification of horse

(54) Shi, Y.; Slaterback, A. F.; Seliskar, C. J.; Heineman, W. R. *Anal. Chem.* **1997**, *69*, 3679–3686.

(55) Shi, Y.; Seliskar, C. J.; Heineman, W. R. *Anal. Chem.* **1997**, *69*, 4819–4827.

(56) DiVirgilio-Thomas, J. M.; Heineman, W. R.; Seliskar, C. J. *Anal. Chem.* **2000**, *72*, 3461–3467.

heart cytochrome *c*, and Carrie Donley for helping with the  $\text{Fc}(\text{COOH})_2$  adsorption experiments.

SUPPORTING INFORMATION AVAILABLE

Band-pass filter spectra, potential-dependent filter spectra, limit of detection, and a comparison of theoretical and experimental

absorbance of adsorbed films. This material is available free of charge via the Internet at <http://pubs.acs.org/ac>.

Received for review August 29, 2002. Accepted December 17, 2002.

AC026086R